ISSN 1063-7761, Journal of Experimental and Theoretical Physics, 2006, Vol. 103, No. 3, pp. 335–345. © Pleiades Publishing, Inc., 2006.
Original Russian Text © D.V. Zhdanov, B.A. Grishanin, V.N. Zadkov, 2006, published in Zhurnal Éksperimental'noĭ i Teoreticheskoĭ Fiziki, 2006, Vol. 130, No. 3, pp. 387–400.

ATOMS, MOLECULES, OPTICS

Orientational Selection of Molecules in Combined Laser and Electrostatic Fields

D. V. Zhdanov, B. A. Grishanin, and V. N. Zadkov

International Laser Center, Moscow State University, Moscow, 119899 Russia

e-mail: zhdanov@comsim1.phys.msu.ru; grishan@comsim1.phys.msu.ru; zadkov@comsim1.phys.msu.ru

Received March 1, 2006

Abstract—It is shown that the combined effects of electrostatic and resonant laser fields on a molecular ensemble can be used to control the orientation of molecules by changing their internal state. In contrast to most other schemes for controlling molecular orientation, the proposed method does not require rotational cooling and can be highly efficient at room temperature.

PACS numbers: 42.50.Hz, 33.80.-b, 82.37.Vb

DOI: 10.1134/S1063776106090019

1. INTRODUCTION

Two- or three-dimensional molecular orientation is a state in which two or three Euler angles are held constant so that the directions of one or all three molecule-fixed coordinate axes are parallel to those of space-fixed coordinate axes. The search for efficient orientation control schemes is stimulated by numerous promising applications in physics, chemistry, and biology and is one of the key aspects of the current development of methods for controlling molecular dynamics [1–13]. In particular, molecular orientation control offers new possibilities for investigating collisional and ionization processes (e.g., see [1, 2]) and stereodynamics of chemical reactions (as in separation of enantiomers by laser distillation [3–10]). Ensembles of oriented molecules are required to deal with various problems in research areas ranging from high-order harmonic generation [11] to quantum computing [12].

Even though this line of research has been developed in numerous studies, orientational control of relatively small molecules remains an open issue. To date, the most detailed studies have been performed on the two-dimensional orientation of such molecules in an external electrostatic field [14–16]. However, this approach can be applied only to strongly polar molecules and is efficient only at very low temperatures, when the energy of electrostatic interaction is comparable to the characteristic rotational energy.

Laser control schemes have proved much more efficient. For example, it was shown theoretically and experimentally in [17–20] that molecules can be two- or three-dimensionally aligned in laser fields. This means that one molecule-fixed coordinate axis or all three of them are collinear with space-fixed ones, respectively, but the molecules may not be arranged in a "head versus tail" order. Laser-induced alignment is feasible as applied to most asymmetric molecules even at room temperature (e.g., see [21]). A detailed review of its applications can be found in [13]. However, molecular orientation cannot be guaranteed in this approach, because the driving forces do not break spatial inversion symmetry.

In [22, 23], it was demonstrated that molecular orientation can be achieved by combining laser and electrostatic fields. In alternative control schemes, including the use of optimized trains of "laser kicks" [24–26] or phase-correlated laser fields [30], inversion symmetry is broken by driving forces that are odd functions of the field strength. Even though such schemes are more efficient than those using purely electrostatic interaction, the requirement of rotational cooling to several kelvins remains their common shortcoming.

This disadvantage is eliminated in the novel approach to molecular orientation control proposed in this paper. Its basic principle is to select molecules that have the required instantaneous orientation rather than simultaneously force all molecules into the target state. Since the oriented molecules are different from the rest of the ensemble by their internal state, they can be treated as a distinct subensemble. As the orientation of the molecules making up the subensemble varies, they are dynamically substituted by others over a characteristic time depending on their rotational frequencies. This laser-driven molecular orientation control scheme can be efficiently used to control processes in which subensembles of this type can be manipulated independently. Therefore, the process dynamics must depend both on the orientation and the initial internal (vibronic) state of the molecules, and the process duration must be much shorter than their free-rotation period. Examples of such processes include ionization, scattering, enantiomer separation, and many other chemical reactions.

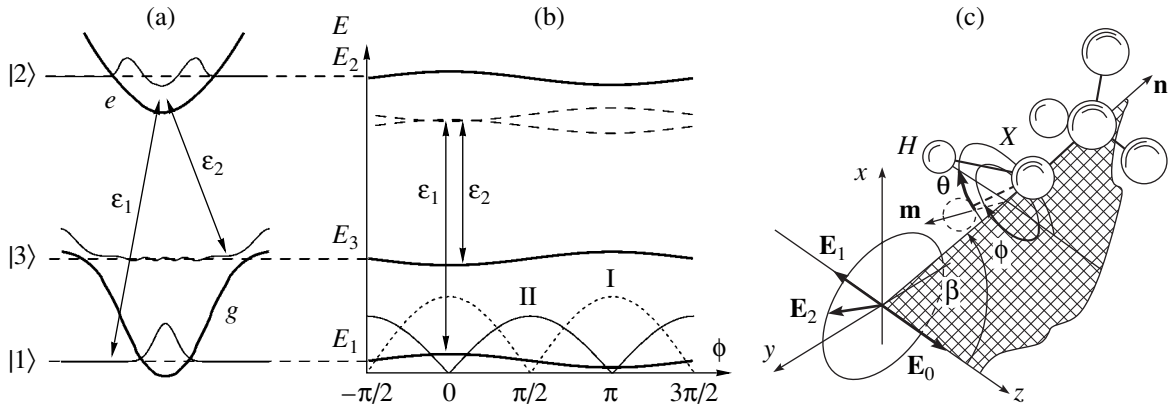

Fig. 1. (a) Schematic diagram of the interaction between a three-level system and laser fields used in the proposed scheme of laser-driven orientational selection. The symmetry of the potential (as depicted here for simplicity) is not at all necessary. (b) Energy levels and laser-induced transitions in the three-state system vs. molecular rotation angle for $\beta = \pi/2$. Separation between dashed curves illustrates the amount of detuning from two-photon resonance. Behavior of $|g_1|$ (I) and $|g_2|$ (II) as functions of ϕ is shown schematically in the bottom part of the panel. (c) Configuration of the polarized fields interacting with a molecule and molecular orientation angles.

The proposed two-dimensional orientation control scheme makes use of the combined effects of electrostatic and laser fields: the laser field transfers populations between vibronic states so that molecules aligned with a space-fixed axis are selected, while the electrostatic field controls orientation by breaking the symmetry between the parallel and antiparallel alignments with the space-fixed axis.

The paper is organized as follows. In Section 2, we present a qualitative analysis of the proposed orientation control scheme. In Section 3, we discuss conditions that must be satisfied by molecular parameters in order to implement efficient control and describe the corresponding class of molecules. In Section 4, we discuss the results of numerical simulations of orientation dynamics. Section 5 summarizes the results of this study and presents the main conclusions.

2. GENERIC SCHEME OF LASER-DRIVEN ORIENTATIONAL SELECTION OF MOLECULES

We consider the problem of selection of molecules with body-fixed axis **m** parallel to the unit basis vector $\mathbf{e}_z$ of a space-fixed coordinate system from a randomly oriented ensemble. Since the selected molecules must be characterized by a small angle $\alpha = \widehat{\mathbf{m}, \mathbf{e}_z}$ between the z axis and the **m** direction, population transfer from the ground vibronic state $|1\rangle$ to an excited vibrational state $|3\rangle$ must be induced when **m** approaches $\mathbf{e}_z$ via thermal rotation, and the reverse process $|3\rangle \longrightarrow |1\rangle$ must occur as the required orientation is lost due to further rotation.

Population can be transferred between the states $|1\rangle$ and $|3\rangle$ by coupling them to a high-lying intermediate vibronic state $|2\rangle$ with laser fields $\mathscr{E}_1$ and $\mathscr{E}_2$, whose frequencies ω_1 and ω_2 are tuned close to resonance with the $|1\rangle \rightleftharpoons |2\rangle$ and $|3\rangle \rightleftharpoons |2\rangle$ transitions, respectively (see Fig. 1a). Since the field-induced coupling depends on the angle between the field polarization vector and the molecular dipole moment, the field–molecule interaction will be modulated by molecular rotation. Therefore, the effect of each field component will be equivalent to that of a pulse train with pulse duration depending on a characteristic rotational frequency. If this frequency is much lower than the Rabi frequencies the laser-induced coupling, then the field–molecule interaction will be an adiabatic process. Under this condition, appropriately polarized laser fields can be used to implement orientation-dependent population transfer between $|1\rangle$ and $|3\rangle$ as a sequential stimulated Raman adiabatic passage [31] that does not involve significant population of the excited state $|2\rangle$.

However, the result of this adiabatic interaction averaged over the rapid field oscillations is symmetric under inversion (orientations with $\alpha = 0$ and π are equally probable). For this reason, an electrostatic field $\mathscr{E}_0$ should also be used to detune the laser field from the two-photon resonance condition for the $|1\rangle \rightleftharpoons |3\rangle$ transition near $\alpha = \pi$ by inducing orientation-dependent Stark shifts and thereby avoid selection of molecules with the undesired orientation.

The objective of this study is to develop an orientation control scheme applicable under normal conditions, when high-lying rotational states are thermally populated even in small molecules. Since these states are characterized by large values of angular momentum, molecular rotations can be described by a classical model.

To simplify analysis, we consider one-dimensional rotation of prolate top molecules, assuming that the molecule-fixed axis **n** is aligned with the principal axis corresponding to the lowest moment of inertia $I_{\min}$. The

corresponding component ν_n of the rotational angular velocity $\boldsymbol{\nu}$ will have the largest value, while the $\mathbf{n}$ axis will rotate with substantially lower angular velocities. Furthermore, we assume that the period of this slow rotation is much longer than the shortest internal relaxation time τ. Under these assumptions, laser-driven molecular dynamics adiabatically follows the time evolution of the $\mathbf{n}$ axis, and the Euler angles specifying its orientation can be treated as parameters independent of other degrees of freedom. The analysis that follows shows that the dynamics of laser-induced orientation is dominated by fast rotations. Accordingly, the dependence on slowly varying Euler angles is taken into account by averaging the dynamics over the Euler-angle distribution for the molecular ensemble, and the only dynamic variable is the angle ϕ of rotation about the $\mathbf{n}$ axis (see Fig. 1c). In this one-dimensional model, free rotation of a molecule is represented as variation of ϕ with a constant frequency ν_n.

The desired selection is achieved when the vectors $\langle 1|\hat{\mathbf{d}}|2\rangle$ and $\langle 3|\hat{\mathbf{d}}|2\rangle$ ($\hat{\mathbf{d}}$ is the dipole moment operator) are aligned with $\mathbf{m}$ and the Stark shifts δE_q ($q = 2, 3$) induced by the static field $\mathscr{E}_0$ relative to the ground-state energy vary with molecular orientation as $\cos\alpha = \sin\beta\cos\phi$,

$$\delta E_q(\mathscr{E}_0, \beta, \phi) = \delta E_q^0(|\mathscr{E}_0|)\sin\beta\cos\phi,$$

where $\beta = (\widehat{\mathbf{e}_z, \mathbf{n}})$ denotes the angle between the $\mathbf{n}$ and z axes (see Fig. 1c). In the next section, we show that the latter condition is satisfied if $\mathscr{E}_0$ is parallel to $\mathbf{e}_z$. The laser field

$$\mathscr{E}_1 = A_1\mathbf{e}_z\cos(\omega_1 t + \varphi_1)$$

must be linearly polarized along $\mathbf{e}_z$, and the field

$$\mathscr{E}_2 = A_2[\mathbf{e}_x\cos(\omega_2 t + \varphi_2) + \mathbf{e}_y\sin(\omega_2 t + \varphi_2)]$$

must be circularly polarized perpendicular to $\mathbf{e}_z$ (see Fig. 1c).

Neglecting the effects due to off-resonant transitions, we write the Hamiltonian for the coupled molecule–field system as

$$\hat{H} = \hat{H}_0 + \hat{H}_0^{\mathrm{I}} + \hat{H}_1^{\mathrm{I}} + \hat{H}_2^{\mathrm{I}}, \tag{1}$$

where

$$\hat{H}_0 = E_1|1\rangle\langle 1| + E_2|2\rangle\langle 2| + E_3|3\rangle\langle 3|$$

is the field-free Hamiltonian with E_p denoting the unperturbed energies of states $|p\rangle$ ($p = 1, 2, 3$). The terms $\hat{H}_0^{\mathrm{I}}$, $\hat{H}_1^{\mathrm{I}}$, and $\hat{H}_2^{\mathrm{I}}$ represent the interaction between the molecule and the electrostatic field $\mathscr{E}_0$ and the laser fields $\mathscr{E}_1$ and $\mathscr{E}_2$:

$$\begin{aligned}\hat{H}_0^{\mathrm{I}}(\mathscr{E}_0, \beta, \phi) &= \delta E_2|2\rangle\langle 2| + \delta E_3|3\rangle\langle 3|,\\ \hat{H}_1^{\mathrm{I}}(\mathscr{E}_1, \beta, \phi) &= H_{1,2}^1|1\rangle\langle 2| + \text{h.c.},\\ \hat{H}_2^{\mathrm{I}}(\mathscr{E}_2, \beta, \phi) &= H_{3,2}^2|3\rangle\langle 2| + \text{h.c.}\end{aligned} \tag{2}$$

where the matrix elements

$$H_{p,r}^i = H_{p,r}^i(\mathscr{E}_i, \beta, \phi) = \langle p|\hat{\mathbf{d}}|r\rangle\mathscr{E}_i$$

characterize the field-induced coupling.

Using the Franck–Condon approximation to describe rovibrational transitions, we rewrite $H_{p,r}^i$ as

$$H_{1,2}^1 = \hbar\Omega_1\mathbf{m}\cdot\mathbf{e}_z\cos(\omega_1 t + \varphi_1),$$

$$H_{3,2}^2 = \hbar\Omega_2\mathbf{m}\cdot[\mathbf{e}_x\cos(\omega_2 t + \varphi_2) + \mathbf{e}_y\sin(\omega_2 t + \varphi_2)],$$

where

$$\Omega_1 = \frac{1}{\hbar}\sqrt{F_{1,2}}\left|A_1(t)\langle g|\hat{\mathbf{d}}|e\rangle_{\mathrm{e}}\right|,$$

$$\Omega_2 = \frac{1}{\hbar}\sqrt{F_{3,2}}\left|A_2(t)\langle g|\hat{\mathbf{d}}|e\rangle_{\mathrm{e}}\right|.$$

Here, $F_{p,r}$ denote Franck–Condon factors, and $\langle g|\hat{\mathbf{d}}|e\rangle_e$ is the reduced dipole transition matrix element between the ground and excited states averaged over the electronic subsystem in the equilibrium nuclear configuration.

Introducing the detunings

$$\Delta_1 = \frac{1}{\hbar}(E_2 - E_1) - \hbar\omega_1,$$

$$\Delta_2 = \frac{1}{\hbar}(E_3 - E_1) - (\omega_1 - \omega_2)$$

and using the rotating-wave approximation, we change from Hamiltonian (1) written in the bare-state basis $\{|1\rangle, |2\rangle, |3\rangle\}$ to the effective Hamiltonian

$$\hat{H}_{\mathrm{eff}} = \begin{pmatrix} 0 & g_1 & 0\\ g_1^* & -\hbar\Delta_1 + \delta E_2 & g_2\\ 0 & g_2^* & -\hbar\Delta_2 + \delta E_3\end{pmatrix}, \tag{3}$$

where

$$g_1 = \frac{1}{2}\hbar\Omega_1 e^{-i\delta_1}\sin\beta\cos\phi,$$

$$g_2 = \frac{1}{2}\hbar\Omega_2 e^{-i\delta_2(\mathbf{n})}(\sin\phi + i\cos\beta\cos\phi)$$

are the complex Rabi frequencies, and δ_1 and δ_2 are constant phase shifts.

First, we analyze the case when the field $\mathcal{E}_0$ is zero, the polarization vector of $\mathcal{E}_1$ lies in the rotation plane ($\beta = \pi/2$ and $\alpha = \phi$), and the exact two-photon resonance condition holds for $|1\rangle \rightleftarrows |3\rangle$ population transfer ($\Delta_2 = 0$). Since no Stark shift is induced, the diagonal elements in (3) are orientation independent, and the Hamiltonian reduces to

$$\hat{H}'_{\text{eff}} = \begin{pmatrix} 0 & g_1 & 0 \\ g_1^* & -\hbar\Delta_1 & g_2 \\ 0 & g_2^* & 0 \end{pmatrix}. \quad (4)$$

Hamiltonian (4) has the eigenvector

$$\psi_d(\phi) = \text{const}\{-e^{-i\delta_1}\Omega_2 \sin\phi, 0, e^{i\delta_2}\Omega_1 \cos\phi\}, \quad (5)$$

which satisfies the condition $(\hat{H}_1^I + \hat{H}_2^I)\psi_d = 0$ and therefore corresponds to a dark state. If the frequency ν_n is not too high, then the molecular state adiabatically follows the evolution of ψ_d. Since $\psi_d(0) = \psi_d(\pi) = \{0, 0, 1\}$ and $\psi_d(\pm\pi/2) = \{1, 0, 0\}$, population is transferred to the state $|3\rangle$ as the rotation angle approaches $\phi = 0$ or π and back to the state $|1\rangle$ as it deviates from these angles.

Laser-driven population transfer between $|1\rangle$ and $|3\rangle$ via a weakly populated intermediate state $|2\rangle$ can be interpreted as a series of sequential processes of stimulated Raman adiabatic passage. Indeed, for a given molecular orientation, the coupling induced by each laser field component is characterized by the absolute value of the corresponding Rabi frequency, $|g_1(t)|$ or $|g_2(t)|$. The curves of $|g_1(t)|$ and $|g_2(t)|$ versus ϕ in Fig. 1b demonstrate that the respective coupling strengths between the molecule and the field components oscillate with period π, vanishing at $\phi = \pm\pi/2$ and $\phi = 0, \pi$ for $\mathcal{E}_1$ and $\mathcal{E}_2$, respectively. Accordingly, the effect of $\mathcal{E}_1$ and $\mathcal{E}_2$ on a molecule rotating about the **n** axis (Fig. 1c) is similar to that of a train of overlapping pulses with a duration of $1/2\nu_n$ whose shape is determined by $|g_1(t)|$ and $|g_2(t)|$. Since population transfer $|1\rangle \longrightarrow |3\rangle$ is induced as $\phi = 0$ or π is approached, the components $\mathcal{E}_1$ and $\mathcal{E}_2$ act as pump and dump (Stokes) pulses, respectively. On the other hand, the simultaneous decrease in $|g_1|$ and increase in $|g_2|$ with ϕ approaching these angles are formally similar to the concurrent growth of the pump field amplitude and decay of the Stokes field amplitude, which are characteristic of stimulated Raman adiabatic passage. As the rotation angle deviates from $\phi = 0$ or π, the roles played by the fields $\mathcal{E}_1$ and $\mathcal{E}_2$ interchange.

It should be noted here that robustness of stimulated Raman adiabatic passage with respect to pulse shape guarantees that the dynamics of laser-driven population transfer is independent of the molecular rotation frequency, provided that the system remains in the adiabatic state throughout the molecule–field interaction.

The above analysis demonstrates that molecules are aligned with the z axis in the case of zero electrostatic field $\mathcal{E}_0$. In a nonzero field $\mathcal{E}_0$, the inversion symmetry of rotation dynamics near $\phi = 0$ and π is broken since the Stark-shifted transition frequencies are orientation dependent. To set up an orientational selection scheme, the laser frequencies ω_1 and ω_2 must be such that the two-photon resonance condition holds for molecules with the desired orientation ($\mathbf{m} \parallel \mathbf{e}_z$),

$$|-\Delta_2 + \delta E_3|_{\phi = 0} = 0, \quad (6)$$

and must be detuned from resonance for molecules with the opposite orientation,

$$|-\Delta_2 + \delta E_3|_{\phi = \pi} = 2|\delta E_3^0| \neq 0.$$

Under these conditions, stimulated Raman adiabatic passage is possible near $\phi = 0$ since the corresponding effective Hamiltonian is similar in form to (4), whereas the population transfer path between $|1\rangle$ and $|3\rangle$ near $\phi = \pi$ is blocked since the system is detuned by $2|\delta E_3^0|$ from the two-photon resonance and ψ_d is therefore not a dark state any longer.

Thus, the orientation corresponding to $\phi = 0$ is guaranteed for a molecule in the vibrational state assembly, at least when β is close to $\pi/2$.

To analyze the selection scheme in more detail, we need estimates for the key parameters of the orientation dynamics. To this end, we specify the class of molecules amenable to this scheme.

3. REQUIREMENTS FOR MOLECULAR PARAMETERS CORRESPONDING TO EFFICIENT LASER-DRIVEN ORIENTATIONAL SELECTION

The assumptions introduced in the foregoing analysis of laser-driven orientational selection of molecules entail the following three conditions for molecular parameters (such as characteristic rotation frequency ν and relaxation time τ) and the states involved in the laser-driven molecular dynamics.

Condition 1. The orientation-dependent difference $|\delta E_3|$ in Stark shift between $|3\rangle$ and $|1\rangle$ must vary as $\cos\alpha$, and its maximum value $|\delta E_3^0|$ measured in units of $\hbar$ must be at least comparable to ν and $1/\tau$.

Condition 2. The transition dipole moments $\langle 1|\hat{\mathbf{d}}|2\rangle$ and $\langle 3|\hat{\mathbf{d}}|2\rangle$ must be collinear with **m**, and their magnitudes must be such that

$$|\langle 1|\hat{\mathbf{d}}|2\rangle \mathbf{E}_1|_{\max} \sim |\delta E_3^0|, \quad |\langle 3|\hat{\mathbf{d}}|2\rangle \mathbf{E}_2|_{\max} \sim |\delta E_3^0|$$

for fields whose amplitudes are so weak that both coupling to other levels and ionization are negligible.

Condition 3. The energies of the states $|1\rangle$, $|2\rangle$, and $|3\rangle$ are separated from the neighboring vibronic energy levels by amounts substantially larger than the rotational energy quantum $\hbar\nu$.

In terms of applicability of the proposed scenario, Condition 1 is the most restrictive one. Indeed, it implies that ν must be sufficiently small, while the change $\delta\mathbf{d}$ in the permanent dipole moment of the molecule associated with $|1\rangle \longrightarrow |3\rangle$ population transfer must be sufficiently large for $|\delta E_3^0|/\hbar$ to be comparable to ν when the electrostatic field is not strong enough to dissociate the molecule. In particular, since the typical change in dipole moment associated with a transition between valence vibrational states does not exceed 0.1 D and electric breakdown occurs under normal conditions when the field strength exceeds 3×10^4 V/cm, it can readily be shown that the selection scenario cannot be implemented for diatomic molecules under normal conditions, because their rotational frequencies are too high ($\nu \sim 10^{11}$ Hz).

A specific class of molecules satisfying the conditions stated above (see Fig. 1c) is characterized as follows. Each molecule contains a hydrogen (or a light metal) atom covalently linked to the rest of the molecule by a highly polar bond with a highly electronegative atom (X in Fig. 1c). The bond must be sufficiently soft to allow torsional motion of the hydrogen atom relative to the rest of the molecule. In mathematical terms, this means that the minimum of the vibrational potential energy U as a function of the torsional angle θ is not very low as compared to the covalent bond energy (see Fig. 1a). For example, these requirements are met for the H_2POSH molecule, where the S–H bond plays the role of the X–H bond described above.

We use a molecule-fixed frame with $\mathbf{m}$ axis pointing in the equilibrium direction of $\overrightarrow{\mathrm{XH}_\sigma}$ in the ground torsional state and define θ as the instantaneous angle $\widehat{\mathbf{m}, \overrightarrow{\mathrm{XH}_\sigma}}$, where $\overrightarrow{\mathrm{XH}_\sigma}$ is the projection of the vector $\overrightarrow{\mathrm{XH}}$ onto the plane σ perpendicular to the torsional axis $\mathbf{n}$.

We note that the eigenstates $|v_l\rangle$ corresponding to low torsional quantum numbers v are localized in the neighborhood of $\theta = 0$, whereas the eigenstates $|v_h\rangle$ with energies near the torsional barrier are localized in the neighborhood of $\theta = \pi$ (see Fig. 1a):

$$\langle v_l|\cos\hat{\theta}|v_l\rangle \approx -\langle v_h|\cos\hat{\theta}|v_h\rangle \approx 1.$$

On the other hand, the v-dependent contribution to the total dipole moment of the molecule is $\mathbf{m}d_0\langle\cos\hat{\theta}\rangle$, where $d_0 = e_{\mathrm{eff}}r_0$, e_{eff} is the effective proton charge, and r_0 is the H–X bond length. Accordingly, the change in molecular dipole moment associated with a $|v_l\rangle \longrightarrow |v_h\rangle$ transition is on the order of $|2d_0|$ in the molecule-fixed frame. Therefore, if the transition time is much shorter than $1/\nu$, then the maximum shift in the $|v_l\rangle \longrightarrow |v_h\rangle$ transition frequency caused by an electrostatic field $\mathscr{E}_0$ can be found by estimating the corresponding change in the molecule's potential energy: $|\Delta U_0|_{\max} \approx 2d_0|\mathscr{E}_0|$.

If the H–X bond length is 1–2 Å, the dissociation limit for the electrostatic field strength is 10–20 kV/cm, and the effective charge is $e_{\mathrm{eff}} \approx |e_0|$ (where e_0 is the electron charge), then we have $|\Delta U_0|_{\max} \approx 1$–$4$ cm^{-1}, which exceeds analogous changes in transitions between electronic or valence vibrational states by one to two orders of magnitude. The corresponding maximum change $\delta(\Delta U_0)_{\max}$ in the energy difference between opposite molecular orientations, $2|\Delta U_0|_{\max} = 4d_0|\mathscr{E}_0|$, is comparable to the characteristic rotational frequency of a medium-sized molecule under normal conditions when $\Delta U_0 = 1$ cm^{-1}. Thus, the states $|v_l\rangle$ and $|v_h\rangle$ satisfy Condition 1 and therefore are promising candidates for $|1\rangle$ and $|3\rangle$, respectively.

It should be noted that, even for a limit strength of $\mathscr{E}_0$ lower than the ionization threshold value, $|\Delta U_0|_{\max}$ is two orders of magnitude lower than the typical thermal energies under normal conditions (~200 cm^{-1}); i.e., the direct effect of $\mathscr{E}_0$ on molecular orientation and torsional motion can be neglected.

For a medium-sized molecule (with a mass on the order of 100 amu and a size on the order of 10 Å), the typical free-rotation frequency is 10^{10}–10^{11} Hz under normal conditions. Since the corresponding rotational quantum number is $J \sim 10^2$, the change in rotational frequency associated with $|1\rangle \rightleftharpoons |3\rangle$ population transfer is smaller than the frequency value by two orders of magnitude. Since no more than two population transfer events can occur during a rotation cycle in the scenario proposed here, we can neglect the change in angular velocity over the rotation period. Moreover, the laser-induced change in the rotational temperature of the ensemble is also negligible, because the characteristic time of significant change in rotational frequency of a molecule is larger than the characteristic collisional relaxation time (about 10^{-10} s) by one to two orders of magnitude.

These estimates justify the analysis of laser-driven orientation dynamics under normal conditions based on the classical treatment of rotations and the assumption of constant rotational frequency. However, for the model of one-dimensional rotation developed in Section 2 to be applicable, the $\mathbf{n}$ axis must be aligned with the principal axis corresponding to the lowest moment

of inertia I_{min} and the remaining two moments of inertia must be much larger than I_{min} (the components of the rotational angular velocity parallel to the corresponding principal axes must be smaller than ν and $1/\tau$).

When the potential $U(\theta)$ is an even function of θ, the vectors $\mathbf{m}$, $\langle 1|\hat{\mathbf{d}}|2\rangle$, and $\langle 3|\hat{\mathbf{d}}|2\rangle$ are collinear only if the states $|2\rangle$ and $|3\rangle$ correspond to even values of v. Furthermore, Conditions 2 and 3 are satisfied only if the Franck–Condon factors for the laser-driven transitions are not too small both in absolute value and in comparison with those for transitions to neighboring states. We note that these requirements are not easy to meet, because a sufficiently large $|\delta E_3^0|$ entails field-induced coupling between states with very different structure and, therefore, very small values of the Franck–Condon factors (10^{-3}–10^{-2}) for the corresponding transitions. Condition 3 can be satisfied if the energy difference between neighboring vibrational states is on the order of tens of inverse centimeters. Since the typical $U(\theta)$ is a slowly varying function and the corresponding well depth is $(1–3)\times 10^3$ cm^{-1}, it can easily be shown that the required energy difference corresponds to torsional motion of the hydrogen atom or a metal atom with atomic mass smaller than 10 amu. The model calculations presented below are performed for the hydrogen atom.

4. SIMULATION OF LASER-DRIVEN ORIENTATIONAL SELECTION

Now, we analyze the efficiency of the proposed selection scheme as applied to molecules of the class described in the preceding section. In numerical estimates, we use the following typical expressions for the vibrational potential energies U_g and U_e of such molecules in the ground and excited electronic states (see Fig. 1):

$$U_e(\theta,\beta,\phi) = hc\left[\frac{3}{2}D_g - [D_e + \Delta D_e(\beta,\phi)]\cos\theta + \frac{1}{2}D_e\cos(2\theta)\right], \quad (7)$$

$$U_g(\theta,\beta,\phi) = hc[D_g - [D_g + \Delta D_g(\beta,\phi)]\cos\theta], \quad (8)$$

where $D_e = 1000$ cm^{-1}, $D_g = 500$ cm^{-1}, and

$$\Delta D_e(\beta,\phi) = \Delta D_g(\beta,\phi) = 2\sin\beta\cos\phi$$

are the orientation-dependent corrections induced by electrostatic field. The numerical values of $\Delta D_e(\beta,\phi)$ and $\Delta D_g(\beta,\phi)$ used here for an X–H bond of length $r_0 \approx 1$ Å and an effective proton charge $e_{eff} \approx |e_0|$ correspond to $|\mathscr{E}_0| = 2\times 10^4$ V/cm.

An analysis of the torsional sublevel structure shows that the best candidates for $|1\rangle$, $|2\rangle$, and $|3\rangle$ by the criteria formulated in Section 3 are the states $|g, 0\rangle$, $|e, 2\rangle$, and $|g, 10\rangle$, respectively, where e and g stand for excited and ground electronic states and the number i refers to the vibrational sublevel v_i. For these states, we have $\delta E^0_{g,0} = -1.87$ cm^{-1}, $\delta E^0_{e,2} = -1.83$ cm^{-1}, $\delta E^0_{g,10} = 1.03$ cm^{-1}, $F_{g,0;e,2} = 0.04$, $F_{g,10;e,2} = 0.014$, and $|\delta E_3^0| \approx 2.9$ cm^{-1}.

The laser field amplitudes are set from the following considerations. The adiabaticity requirement implies that the effective pump and dump pulse areas must be much larger than π, whereas the population transfer path to $|g, 10\rangle$ can be effectively blocked near $\phi = \pi$ only if $|\Omega_i| \ll |\delta E_3^0|$ ($i = 1, 2$). Since the Stark shifts δE^0 are comparable to $h\nu_n$ (recall that this quantity determines the effective pulse durations), both requirements cannot be met simultaneously. For this reason, the amplitudes are set to satisfy the condition $\Omega_i \lesssim |\delta E_3^0|/2$: $A_1 = 6\times 10^7$ V/m and $A_2 = 2\times 10^8$ V/m. These settings correspond to moderate laser intensities on the order of 10^9 W/cm^2.

The laser frequencies ω_1 and ω_2 are set to optimize the detunings Δ_1 and Δ_2. The optimal value of Δ_2 is determined by condition (6): $\Delta_2 \approx \delta E_3^0 = -2.75$ cm^{-1}. Since dark state (5) is independent of Δ_1, the value of this parameter is not essential under adiabatic conditions. However, even though the undesired contribution of nonadiabatic processes vanishes in the limit of $\Delta_1 \gg \delta E_3^0$, an increase in Δ_1 entails stronger coupling to other vibrational states, and a higher field intensity is required to maintain adiabaticity. For this reason, we set $\Delta_1 \approx -3\delta E_3^0 = 8.2$ cm^{-1} as an optimal value. Because of the Stark shifts, the laser frequencies ω_1 and ω_2 are detuned from resonance by amounts varying within 8.39–8.08 and 8.24–13.2 cm^{-1}, respectively. Note that the amplitude A_2 is taken three times larger than A_1, because the maximum difference in detuning is approximately twofold, while the Franck–Condon factor for the $|g, 0\rangle \rightleftharpoons |e, 2\rangle$ transition is smaller than that for the $|e, 2\rangle \rightleftharpoons |g, 10\rangle$ transition by a factor of 1.5.

Thus, the efficiency of orientational selection cannot be reliably evaluated for the class of molecules considered here by approximately treating laser-driven orientation dynamics under normal conditions as adiabatic passage in a three-state system, because nonadiabatic coupling effects cannot be completely eliminated and off-resonant interactions must be taken into account at high laser intensities. For this reason, we consider an augmented system with five neighboring vibrational levels above and five below each of the original three

levels. Laser-driven dynamics is simulated by using the classical model of a one-dimensional rigid rotor developed above, and vibronic transitions are computed by solving the Lindblad equation

$$\frac{d}{dt}\hat{\rho} = -\frac{i}{\hbar}[\hat{H}, \hat{\rho}] + \mathcal{L}_r\hat{\rho} \quad (9)$$

for the density matrix $\hat{\rho}$, where Hamiltonian (1) is used with expressions (2) written in the augmented (vibronic) basis, and the last term represents relaxation.

The relaxation processes playing the dominant role in the laser-driven dynamics are collisional relaxation and internal conversions. To simplify numerical simulations, we assume that only longitudinal relaxation to the ground state $|g, 0\rangle$ is essential, with equal relaxation times τ for all of the excited states. Under this assumption,

$$\mathcal{L}_r\hat{\rho} = \frac{1}{\tau}[(\mathrm{Tr}\hat{\rho})|g, 0\rangle\langle g, 0| - \hat{\rho}].$$

In the standard rotating-wave approximation (RWA), Eq. (9) is rewritten for the transformed density matrix

$$\hat{\rho}_{\mathrm{RWA}} = \exp\left(\frac{i}{\hbar}\hat{H}_0 t\right)\hat{\rho}\exp\left(-\frac{i}{\hbar}\hat{H}_0 t\right)$$

as

$$\frac{d}{dt}\hat{\rho}_{\mathrm{RWA}} = -\frac{i}{\hbar}[\hat{H}_{\mathrm{RWA}}, \hat{\rho}_{\mathrm{RWA}}] + \frac{1}{\tau}[(\mathrm{Tr}\hat{\rho}_{\mathrm{RWA}})|g, 0\rangle\langle g, 0| - \hat{\rho}_{\mathrm{RWA}}]. \quad (10)$$

This equation is formally similar to (9), except that the interaction Hamiltonian $\hat{H}_{\mathrm{RWA}}$ (depending on time as a function of $\phi(t)$: $\phi(t) = \nu_n t + \phi(0)$) is substituted for $\hat{H}$. According to (10), the evolution of $\hat{\rho}_{\mathrm{RWA}}(t)$ can be approximately computed by using the expression

$$\hat{\rho}_{\mathrm{RWA}}(t + \Delta t) = U\left(\phi\left(t + \frac{\Delta t}{2}\right)\right) \times \hat{\rho}_{\mathrm{RWA}}(t)U\left(\phi\left(t + \frac{\Delta t}{2}\right)\right)^{-1} + \frac{\Delta t}{\tau}[(\mathrm{Tr}\hat{\rho}_{\mathrm{RWA}})|g, 0\rangle\langle g, 0| - \hat{\rho}_{\mathrm{RWA}}(t)], \quad (11)$$

with

$$U(\phi) = \exp\left(-\frac{i}{\hbar}\hat{H}_{\mathrm{RWA}}\Delta t\right),$$

which is derived by dropping $O((\Delta t)^2)$ terms. For each particular value of β and ν_n, the evolution was computed by substituting tabular values of $U(\phi)$ calculated with a step of 1.1° or 5° into (11).

The efficiency of orientational selection is quantified by the direction cosine $\langle\cos\alpha\rangle_{g,10} = \langle\sin\beta\cos\phi\rangle_{g,10}$, where the averaging is performed only over the molecules in the vibronic state $|3\rangle = |g, 10\rangle$.

Following the qualitative analysis presented above, we begin with the case of $\beta = \pi/2$ and examine the $|g, 0\rangle$ and $|g, 10\rangle$ populations as functions of the initial orientation and rotational frequency of a molecule. Some important features of the dynamics are elucidated by neglecting the relaxation term. Consider a molecule in the ground state $|g, 0\rangle$ freely rotating about the **n** axis before $t = 0$. Suppose that both electrostatic and laser fields are turned on at $t = 0$. Generally, the behavior of the molecule at $t > 0$ depends on ν_n and $\phi(t = 0)$ and determines its state corresponding to $\phi = \phi_0$. To gain a clearer understanding, we examine the dependence of the molecular state on as functions of the period T and the total phase Φ gained after $t = 0$.

Figure 2 shows the populations $\langle g, 0|\hat{\rho}|g, 0\rangle$, $\langle g, 10|\hat{\rho}|g, 10\rangle$, and $\langle e, 2|\hat{\rho}|e, 2\rangle$ as functions of Φ and ϕ_0 computed for $\nu_n = 4 \times 10^{10}$ Hz and a particular direction of rotation. One can see that the molecules remain in the ground state $|g, 0\rangle$ most of the time. Only when ϕ lies within a relatively narrow interval of width about $\pi/2$ centered at $\phi = 0$, the population is almost completely transferred to the excited state $|g, 10\rangle$, with the exception of the molecules for which ϕ is close to 0 at $t = 0$. These molecules also exhibit adiabatic behavior corresponding to the evolution of some highly excited dressed state in the absence of relaxation. These molecules are responsible for the dominant contribution to the population of the excited electronic state. It should be noted that nonadiabatic field–molecule interactions significantly contribute to the dynamics even at the rotational frequency specified above, as manifested by small-scale wavelike variation of the state populations as functions of Φ. Nevertheless, the efficiency of orientational selection is fairly high: $\langle\cos\phi\rangle_{g,10} = 0.17$.

When relaxation is taken into account, the dependence on the initial molecular orientation becomes weaker, and the contrasting pattern illustrated by Fig. 2 tends to smear out as a steady-state regime is approached in the limit of $\Phi \gg \tau\nu$. The dependence of the dynamic behavior of the coupled molecule–field system on rotational frequency and relaxation is illustrated by Fig. 3, where the instantaneous $|g, 10\rangle$ populations corresponding to $\phi = 0$ and π are shown versus T for $\tau = 10^{-10}$ s (collisional relaxation time under normal conditions) and $\tau = 10^{-11}$ s.

According to Fig. 3, when the rotation period is small, nonadiabatic coupling effects play a dominant role and the dynamics are determined by the effective

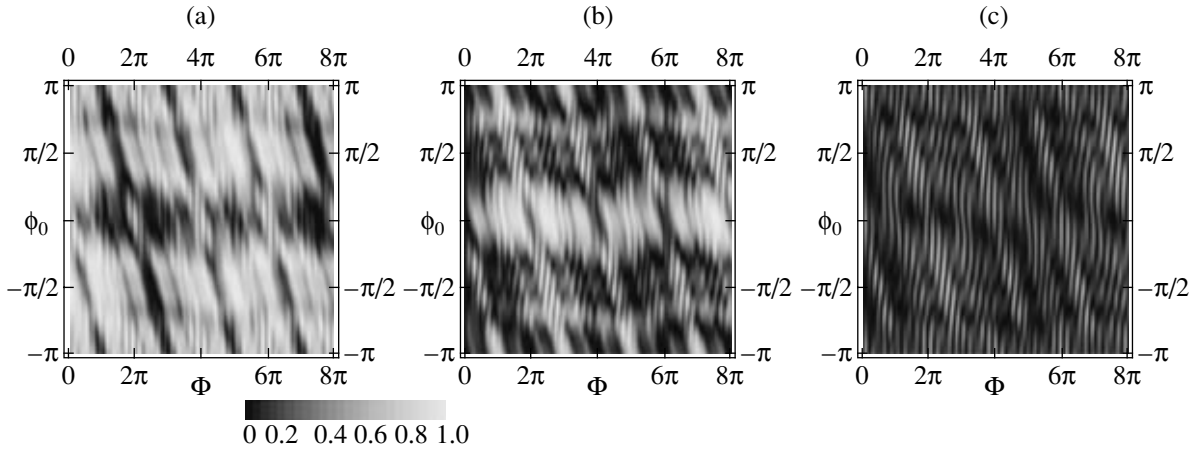

Fig. 2. Populations of the states $|g, 0\rangle$ (a), $|g, 10\rangle$ (b), and $|e, 2\rangle$ (c) as functions of Φ and ϕ_0 for $\nu_n = 4 \times 10^{10}$ Hz and $\beta = \pi/2$ in the absence of relaxation. Inset: grayscale calibration bar.

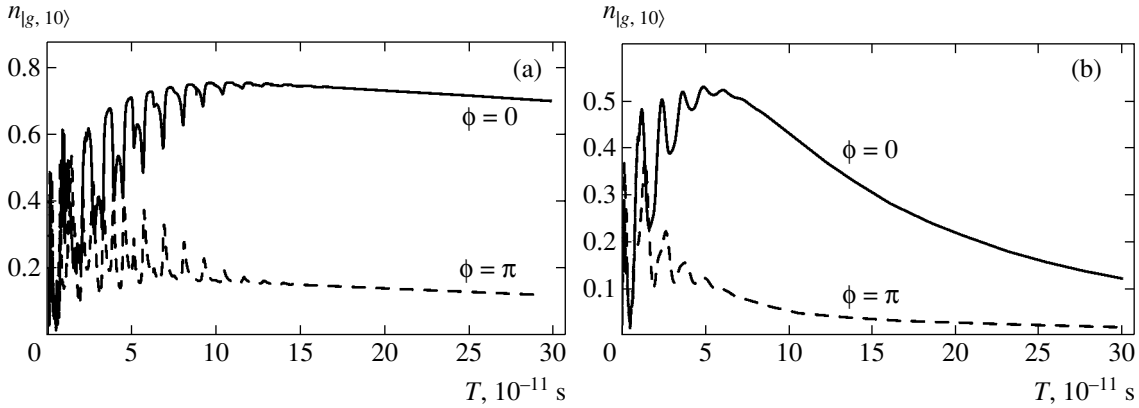

Fig. 3. Steady-state $|g, 10\rangle$ populations for $\phi = 0$, π and $\beta = \pi/2$ vs. molecular rotation period for (a) $\tau = 10^{-10}$ s (slow relaxation) and (b) $\tau = 10^{-11}$ s (fast relaxation).

Rabi frequency for the $|g, 0\rangle \longrightarrow |g, 10\rangle$ population transfer and by the corresponding effective pulse area S. Since the pulse area is proportional to T, the populations exhibit pronounced oscillatory behavior at small T. However, when $T \approx 3 \times 10^{-11}$ s, the contribution of adiabatic processes is sufficiently large for the $|g, 10\rangle$ population to exhibit stable behavior as a function of orientation; i.e., orientational selection of molecules becomes possible.

Furthermore, an analysis shows that the spurious population of the excited state $|e, 2\rangle$ decreases with increasing T. Comparing the graphs presented in Fig. 3, we see that relaxation has a mixed effect on the efficiency of orientational selection. On the one hand, the $|g, 10\rangle$ population substantially decreases with τ when T is large; i.e., relaxation impedes orientation. On the other hand, when τ is relatively large (see Fig. 3a), the adiabatic behavior is mitigated for fast-rotating molecules (with $T < 4 \times 10^{-11}$ s) by the Rabi oscillations developing as a result of stronger nonadiabatic field–molecule coupling. It is clear from Fig. 3b that efficiency of orientational selection improves decreasing τ as nonadiabatic processes are increasingly suppressed. Note that orientational selection can be efficient even if the Rabi frequency for the two-photon process is on the order of $\nu_n/4$ (which corresponds to $T \approx 3 \times 10^{-11}$ s). Thus, when τ is sufficiently small, an appreciable efficiency of laser-driven orientational selection should be achieved even if the Rabi frequency is comparable to the characteristic rotational frequency.

Quantitative analysis under experimentally realistic conditions requires three-dimensional simulation of molecular rotations (without the constraint $\beta = \pi/2$). We performed computations of this kind, assuming that the **n** axis of the molecule is aligned with its principal axis corresponding to the lowest moment of inertia $I_{\min}$ and the remaining two moments of inertia are much larger than $I_{\min}$, so that the components of the rotational angular velocity parallel to the corresponding principal axes are smaller than ν or $1/\tau$. Under these assumptions, the

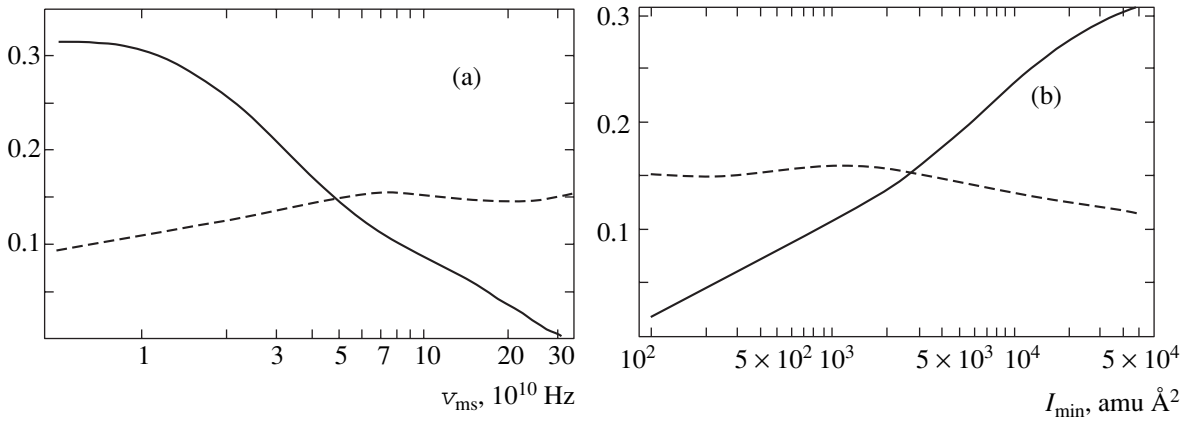

Fig. 4. Plots of $\langle\cos\alpha\rangle_{g,\,10}$ (solid curves) and normalized $|g, 10\rangle$ population (dashed curves) averaged over an ensemble of randomly oriented molecules in rotational thermal equilibrium vs. rms rotational frequency ν_{ms} (a) and moment of inertia I_{min} at $T_{rot} = 300$ K (b). Computations were performed by assuming that the moments of inertia other than I_{min} are higher than 10^3 amu Å^2.

model of one-dimensional rotation can be applied. To facilitate analysis in this approximation and take into account possible detrimental effects of internal conversions (which are generally strong in polyatomic molecules), we set $\tau = 10^{-11}$ s. The remaining molecular and field parameters are similar to those used in the simulations presented above.

To examine the dependence of the efficiency of orientational selection on the **n** direction and rotational frequency, we computed laser-driven orientation dynamics for several values of T and β and calculated $\langle\cos\alpha\rangle_{g,\,10}$ and normalized $|g, 10\rangle$ population as functions of these parameters. The values of T and β were varied with steps of 2.5×10^{-13} s and $\pi/20$, respectively. We took into account the fact that the laser-driven dynamics depends not only on the rotational frequency, but also on the direction of rotation about the **n** axis, which is related to the helicity of the circularly polarized beam $\mathscr{E}_2$.

An analysis of the computed dependence of $\langle\cos\alpha\rangle_{g,\,10}$ on T and β shows that it is qualitatively different for ν_n above and below the threshold frequency $\nu_{tr} = 4 \times 10^{10}$ Hz corresponding to $T = 2.5 \times 10^{-11}$ s. When $\nu_n < \nu_{tr}$, absolute values of $\langle\cos\alpha\rangle_{g,\,10}$ as high as 0.45 are reached. Its weak dependence on ν_n is indicative of adiabatic nature of field–molecule interaction. When $T > 2.5 \times 10^{-11}$ s, both efficiency of orientational selection and time-averaged $|g, 10\rangle$ population tend to decrease with ν_n because of an increasing effect of relaxation processes. When $\nu_n > \nu_{tr}$, the field–molecule interaction is an essentially nonadiabatic process: both the absolute value and sign of $\langle\cos\alpha\rangle_{g,\,10}$ exhibit oscillatory behavior as functions of the rotation period and, hence, of the effective pulse area. Moreover, strong dependence on the direction of rotation (sign of ν_n) is observed: the absolute value of ν_n corresponding to $T \sim 1.5 \times 10^{-11}$ s is comparable to Δ_1 and Δ_2 and is approximately equal to half the Rabi frequency for the two-photon transition. This explains the fact that the time-averaged $|g, 10\rangle$ population reaches a maximum in the neighborhood of this value of T. Accordingly, molecules with $T = (1–2) \times 10^{-11}$ s are responsible for the dominant detrimental effect on the selection process.

The computed dependence of $\langle\cos\alpha\rangle_{g,\,10}$ and $|g, 10\rangle$ population on T and β is used to calculate $\langle\cos\alpha\rangle_{g,\,10}$ and normalized $|g, 10\rangle$ population averaged over an ensemble of randomly oriented molecules in rotational thermal equilibrium. In this case, which is the most realistic in terms of experimental implementation,[1] the distribution of molecules over $|\nu_n|$ can be written as

$$\rho_T(|\nu_n|) = \frac{2}{\sqrt{2\pi}\nu_{ms}}\exp\left(-\frac{\nu^2}{2\nu_{ms}^2}\right),$$

with rms frequency ν_{ms} of rotation about the **n** axis calculated as

$$\nu_{ms} = \frac{1}{2\pi}\sqrt{\frac{kT_{rot}}{I_{min}}}, \qquad (12)$$

where T_{rot} is the rotational temperature and k is Boltzmann's constant.

Figure 4 shows the calculated results. Since analysis of the efficiency of the proposed scheme of laser-driven orientational selection under normal conditions is of primary interest, the results for $T_{rot} = 300$ K are shown in the right panel of Fig. 4 as functions of I_{min} calculated by using (12) and assuming that the other two moments of inertia are higher than 1000 amu Å^2. The most remarkable features observed here are the following.

[1] Thermal population of vibrational excited states is neglected.

The relatively large value of normalized $|g, 10\rangle$ population varying between 0.10 and 0.15 over the examined interval of $I_{\min}$ demonstrates the high efficiency of the proposed scenario regardless of the dimensions and mass of molecules (at least 10% of the total number of molecules in the ensemble reside in the target state).

Furthermore, the ensemble-averaged value of $\langle\cos\alpha\rangle_{g,10}$ exceeding 0.1 for molecules with $I_{\min}$ = 900 amu Å^2 under normal conditions suggests that the efficiency of orientational selection is fairly high even for relatively light (fast-rotating) molecules.

It should be noted that the highest ensemble-averaged value of $\langle\cos\alpha\rangle_{g,10}$ attainable in the parameter domain considered here is approximately 0.3. Apart from relaxation processes, the factors responsible for this relatively low efficiency include the impossibility of strictly adiabatic passage for typical light molecules. It should also be kept in mind that the highest rate of adiabatic population transfer between the ground and target states corresponds to the overlap of the effective pump and dump pulses. In the proposed scenario, this occurs when $\alpha \approx \pi/4$ (see Fig. 1b). Therefore, the molecules in the state $|g, 10\rangle$ are mainly those whose **m** axes lie within the relatively wide cone $\{0 \le \alpha \le \pi/4\}$. Moreover, when $T \gtrsim \tau$, the detrimental effect of relaxation processes leads to deviation of the maximum of $|g, 10\rangle$ from the optimal orientation ($\alpha = 0$) into the interval of strongest field–molecule interaction ($\alpha \approx \pi/4$). For this reason, the unattainability of orientational selection efficiency close to unity is an inherent shortcoming of the proposed scheme.

5. CONCLUSIONS

The proposed scenario of laser-driven orientational selection of molecules may prove to be one of the most promising schemes for controlling rotational dynamics of molecular ensembles. The key advantage of the scheme, as compared to various molecular orientation scenarios of inversion symmetry breaking, is the high efficiency of control at rotational temperatures of up to 300 K even for light molecules with masses on the order of 100 amu and characteristic dimensions of about 5 Å. Moreover, since the desired result is achieved without using any special procedure for optimizing laser fields (such as amplitude modulation or phase matching between the field components), an additional advantage of the proposed scheme, as compared to scenarios involving optimal control and pulsed laser fields, is the relative simplicity of experimental implementation. Yet another advantage lies in the fact that effective selection is achieved by using laser beams of moderate intensity (~10^9 W/cm^2) and persists as long as the laser and electrostatic fields are applied.

The principal requirement is that the molecule must contain an isolated bond between a highly electronegative atom and a hydrogen (or light metal) that is sufficiently soft to allow torsional motion of the hydrogen atom. Since bonds of this type are frequent in both organic and inorganic molecules, the proposed orientational selection scheme is applicable to a broad class of molecules.

It would be interesting to explore the possibility of using the present selection scheme in conjunction with the scheme of orientational control by means of a multimode laser field proposed in [30]. We expect that this setting will obviate the use of electrostatic field and provide a basis for designing orientational control scenarios that would be effective as applied to almost every asymmetric molecule at high rotational temperatures.

ACKNOWLEDGMENTS

This work was supported by the Russian Foundation for Basic Research, project no. 04-02-17554.

REFERENCES

1. B. Friedrich, H.-G. Rubahn, and N. Sathyamurthy, Phys. Rev. Lett. **69**, 2487 (1992).
2. A. Saenz, Phys. Rev. A **66**, 063407 (2002).
3. L. González, K. Hoki, D. Kröner, et al., J. Chem. Phys. **113**, 11134 (2000).
4. A. S. Leal, D. Kröner, and L. González, Eur. Phys. J. D **14**, 185 (2001).
5. K. Hoki, Y. Ohtsuki, and Y. Fujimura, J. Chem. Phys. **114**, 1575 (2001).
6. M. Shapiro, E. Frishman, and P. Brumer, Phys. Rev. Lett. **84**, 1669 (2000).
7. L. González, D. Kröner, and I. R. Sola, J. Chem. Phys. **115**, 2519 (2001).
8. K. Hoki, L. González, and Y. Fujimura, J. Chem. Phys. **116**, 2433 (2002).
9. Y. Ohta, K. Hoki, and Y. Fujimura, J. Chem. Phys. **116**, 7509 (2002).
10. K. Hoki, L. González, and Y. Fujimura, J. Chem. Phys. **116**, 8799 (2002).
11. R. Velotta, N. Hay, M. B. Mason, et al., Phys. Rev. Lett. **87**, 183901 (2001).
12. E. A. Shapiro, I. Khavkine, M. Spanner, and M. Ivanov, Phys. Rev. A **67**, 013406 (2003).
13. H. Stapelfeldt and T. Seideman, Rev. Mod. Phys. **75**, 543 (2003).
14. J. M. Rost, J. C. Griffin, B. Friedrich, and D. R. Herschbach, Phys. Rev. Lett. **68**, 1299 (1992).
15. R. Gonzalez-Ferez and P. Schmelcher, Phys. Rev. A **69**, 023402 (2004).
16. P. A. Block, E. J. Bohac, and R. E. Miller, Phys. Rev. Lett. **68**, 1303 (1992).
17. B. Friedrich and D. R. Herschbach, Phys. Rev. Lett. **74**, 4623 (1995).
18. Ch. Ellert and P. B. Corkum, Phys. Rev. A **59**, 3170 (1999).

19. J. J. Larsen, K. Hald, N. Bjerre, et al., Phys. Rev. Lett. **85**, 2470 (2000).
20. J. G. Underwood, B. J. Sussman, and A. Stolow, Phys. Rev. Lett. **94**, 143002 (2005).
21. G. Ravindra Kumar, P. Gross, C. P. Safvan, et al., J. Phys. B **29**, L95 (1996).
22. H. Sakai, S. Minemoto, H. Nanjo, et al., Phys. Rev. Lett. **90**, 083001 (2003).
23. H. Tanji, S. Minemoto, and H. Sakai, Phys. Rev. A **72**, 063401 (2005).
24. L. Cai, J. Marango, and B. Friedrich, Phys. Rev. Lett. **86**, 775 (2001).
25. D. Sugny, A. Keller, O. Atabek, et al., Phys. Rev. A **69**, 043407 (2004).
26. D. Sugny, A. Keller, O. Atabek, et al., quant-ph/0310099.
27. D. Sugny, A. Keller, O. Atabek, et al., quant-ph/0510008.
28. D. Sugny, A. Keller, O. Atabek, et al., quant-ph/0510114.
29. K. Hoki and Y. Fujimura, Chem. Phys. **267**, 187 (2001).
30. S. Guerin, L. P. Yatsenko, H. R. Jauslin, et al., Phys. Rev. Lett. **88**, 233601 (2002).
31. K. Bergmann, H. Theuer, and B. W. Shore, Rev. Mod. Phys. **70**, 1003 (1998).

Translated by A. Betev